

Effects of the radial flows on the chemical evolution of the Milky Way disk

E. Spitoni^{1,3} * and F. Matteucci^{1,2}

¹ Dipartimento di Astronomia, Università di Trieste, via G.B. Tiepolo 11, I-34131, Trieste, Italy

² I.N.A.F. Osservatorio Astronomico di Trieste, via G.B. Tiepolo 11, I-34131, Trieste, Italy

³ Department of Mathematics, University of Évora, R. Romão Ramalho 59, 7000 Évora, Portugal

Received xxxx / Accepted xxxx

ABSTRACT

Context. The majority of chemical evolution models assume that the Galactic disk forms by means of infall of gas and divide the disk into several independent rings without exchange of matter between them. However, if gas infall is important, radial gas flows should be taken into account as a dynamical consequence of infall.

Aims. The aim of this paper is to test the effect of radial gas flows on detailed chemical evolution models (one-infall and two-infall) for the Milky Way disk with different prescriptions for the infall law and star formation rate.

Methods. We modified the equation of chemical evolution to include radial gas flows according to the method described in Portinari & Chiosi

Results. We found, that with a gas radial inflow of constant speed the metallicity gradient tends to steepen. Taking into account a constant time scale for the infall rate along the Galaxy disk and radial flows with a constant speed, we obtained a too flat gradient, at variance with data, implying that an inside-out formation and/or a variable gas flow speed are required. To reproduce the observed gradients the gas flow should increase in modulus with the galactocentric distance, both in the one-infall and two-infall models. However, the inside-out disk formation coupled with a threshold in the gas density (only in the two-infall model) for star formation and/or a variable efficiency of star formation with galactocentric distance can also reproduce the observed gradients without radial flows.

Conclusions. We showed that the radial flows can be the most important process in reproducing abundance gradients but only with a variable gas speed. Finally, one should consider that uncertainties in the data concerning gradients prevent us to draw firm conclusions. Future more detailed data will help to ascertain whether the radial flows are a necessary ingredient in the formation and evolution of the Galactic disk and disks in general.

Key words. Galaxy: abundances - Galaxy: evolution - Galaxy: disk - Stars: supernovae: general

1. Introduction

Generally, a good agreement between model predictions and observed properties of the Galaxy is obtained by models which assume that the disk formed by infall of gas: (e.g Matteucci & François (1989), Chiappini et al. 1997, François et al. 2004).

The formation timescale of the thin disk is assumed to be a function of the galactocentric distance, leading to an inside-out scenario for the Galaxy disk build-up (Matteucci & François 1989). This assumption helps in reproducing the abundance gradients along the disk as shown in studies such as Chiappini et al. (2001), Cescutti et al. (2007), Colavitti et al. (2009) and Marcon-Uchida et al. (2010). In these papers were analyzed the parameter space of the “static” chemical evolution models considering different infall and star formation (SF) rate laws in order to reproduce the observed abundance gradients. Cescutti et al. (2007) showed that the results obtained using a chemical evolution model with a two-infall law and inside-out formation

are in very good agreement with the data on Cepheids in the galactocentric distance range 5-17 kpc for many of the studied elements.

Colavitti et al. (2009) found that it is impossible to fit all the disk constraints at the same time without assuming an inside-out formation for the Galactic disk together with a threshold in the gas density for the SF rate. In particular, the inside-out formation is important to reproduce the right slope of the abundance gradients in the inner disk, whereas the threshold gas density is important to reproduce present day gradients in the outer disk. Generally, simple models without radial gas flows and with a radially constant formation timescale cannot reproduce the slope in the inner disk. In the framework of models with no inside-out mechanism such as the model with the cosmological infall law of Colavitti et al. (2009) they tested the effect of the efficiency of SF varying with the galactocentric radius, being higher in the innermost than in the outermost regions of the Galactic disk. This assumption, even without the threshold in the surface gas density, can produce gradients

* email to: spitoni@oats.inaf.it

with the right slope both in the inner and outer regions of the Galactic disk but it fails in reproducing the gas density distribution along the disk. However, if gas infall is important, the Galactic disk is not adequately described by a simple multi-zone model with separated zones (Mayor & Vigroux 1981). To maintain consistency, radial gas flows have to be taken into account as a dynamical consequence of infall. The infalling gas has a lower angular momentum than the circular motions in the disc, and mixing with the gas in the disc induces a net radial inflow. Lacey & Fall (1985) estimated that the gas inflow velocity is up to a few km s^{-1} . Goetz & Köppen (1992) studied numerical and analytical models including radial flows. They concluded that radial flows alone cannot explain the abundance gradients but are an efficient process to amplify the existing ones. In particular, they suggested that the speed of the flow should increase with galactocentric distance and only change by 0.15 km s^{-1} per kpc, well below any detection limit for drift velocities of molecular clouds. Portinari & Chiosi (2000) implemented in the detailed chemical evolution model of Portinari & Chiosi (1999), characterized by a single infall episode, the effects of radial gas inflows by means of the following assumptions:

- an uniform inflow pattern through the disk, with speed $v_R = -1 \text{ km s}^{-1}$ applied to a model with a Schmidt (1959) SF law and they found, as expected, that the metallicity gradient tends to steepen in the presence of radial gas flows;
- they considered models with various SF laws and tuned the inflow velocity pattern, in each case, as to match the observational data relative to the radial profiles of the Galactic disk. They suggested that inclusion of radial flows in the chemical models can improve the match with the data. For these models the radial velocities span the range $-1 \leq v_R \leq -0.3 \text{ km s}^{-1}$.

In the work of Schönrich & Binney (2009) both the stellar and gas flow were considered in a chemical evolution model without inside-out formation. They are able to reproduce the observed data considering a variable speed of the gas flow in the range 0 km s^{-1} to -5 km s^{-1} .

Another physical cause of radial flows is the gas viscosity. Viscosity in the gas layers induces radial inflows in the inner parts of the disc and outflows in the outer parts, with velocities of $\sim 0.1 \text{ km s}^{-1}$ (Lacey & Fall 1985). Thon & Meusinger (1998) presented a model for the chemical and dynamical evolution of the Galactic disk which combines viscous radial gas flows with infall of external gas onto the disk, and infall-induced radial gas flows. In this hydrodynamic “hybrid” model it was assumed that the viscosity of the gas is closely related to the processes of SF and the energetic response from massive stars, i.e. the timescales for viscous transport and for gas consumption by SF are nearly the same. Following the parameterization of Sommer-Larsen & Yoshii (1989), they obtained a SF rate law depending on the viscosity parameters.

Gravitational interactions between gas and spiral density waves lead to large-scale shocks, dissipation and therefore radial inflows of gas (or outflows in the outer parts) with typical velocities of $\sim 0.3 \text{ km s}^{-1}$ (e.g. Bertin & Lin 1996 and references therein); much larger velocities can be achieved in the

inner few kpc in the presence of a barred potential. However, given the small values of the flow speed in these works, the effect on the abundance gradients are negligible.

In this work we include radial inflows in 2 different chemical evolution models: a one-infall and a two-infall model. In particular, this is the first time that radial flows are included in the two-infall model. We test a constant velocity pattern for the radial inflow as well as a best fit pattern as done in Portinari & Chiosi (2000). We then study the effect of radial flows on the formation of gradients coupled with the inside-out mechanism formation and the effect of the threshold in the SF. Last but not least, we compare our results with the most recent data now available, including Cepheids, and this represents a novelty relative to previous works. This comparison will allow us to put constraints on the mechanisms of gradient formation.

The paper is organized as follows: in Sect. 2 we describe the reference “static” models used in this work, in Sect. 3 we report the nucleosynthesis prescriptions, in Sect. 4 we present the implementation of the radial inflow of gas in a detailed chemical evolution model, in Sect. 5 observational data are shown. In Sect. 6 we report and discuss our results. Finally we draw the main conclusions in Sect. 7.

2. The chemical evolution model for the Milky Way

In order to reproduce the chemical evolution of the thin-disk, we adopt as a reference model an updated one-infall version of the chemical evolution model presented by Matteucci & François (1989). In this model, the galactic disk is divided into several concentric rings which evolve independently without exchange of matter.

The infall law for the thin-disk is defined as:

$$B(r, t) = b(r)e^{-t/\tau_D}, \quad (1)$$

where τ_D is the timescale for the infalling gas into the thin-disk. It is worth noting that eq.(1) differs from the two-infall model of Chiappini et al. (1997) which assumes an infall law such as:

$$A(r, t) = a(r)e^{-t/\tau_H(r)} + b(r)e^{-(t-t_{\max})/\tau_D(r)}. \quad (2)$$

To have an inside-out formation on the disk, the timescale for the mass accretion is assumed to increase with the Galactic radius following a linear relation given by (see Chiappini et al. 1997):

$$\tau_D = 1.033r(\text{kpc}) - 1.27 \text{ Gyr}, \quad (3)$$

for galactocentric distances $\geq 4 \text{ kpc}$. The region within 4 kpc is not considered in this paper and has by the strict inflow no impact on the outer regions. The coefficient $b(r)$ is obtained by imposing a fit to the observed current total surface mass density in the thin disk as a function of the galactocentric distance given by:

$$\sigma(r) = \sigma_D e^{-r/r_D}, \quad (4)$$

where $\sigma_D = 531 M_\odot \text{ pc}^{-2}$ is the central total surface mass density and $r_D = 3.5 \text{ kpc}$ is the scale length.

In order to make the program as simple and generalized as possible, we used a SF rate proportional to a Schmidt (1959) law:

$$\psi(r, t) \propto \nu \Sigma_{gas}^k(r, t) \quad (5)$$

where ν is the efficiency in the SF process and the surface gas density is represented by $\Sigma_{gas}(r, t)$ while the exponent k is equal to 1.4 (see Kennicutt 1998).

The equation below describes the time evolution of G_i , namely the mass fraction of the element i in the gas:

$$\begin{aligned} \dot{G}_i(r, t) = & -\psi(r, t)X_i(r, t) \\ & + \int_{M_L}^{M_{Bm}} \psi(r, t - \tau_m) Q_{mi}(t - \tau_m) \phi(m) dm \\ & + A_{Ia} \int_{M_{Bm}}^{M_{BM}} \phi(M_B) \cdot \left[\int_{\mu_m}^{0.5} f(\mu) \psi(r, t - \tau_{m2}) Q_{mi}^{SNIa}(t - \tau_{m2}) d\mu \right] dM_B \\ & + (1 - A_{Ia}) \int_{M_{Bm}}^{M_{BM}} \psi(r, t - \tau_m) Q_{mi}(t - \tau_m) \phi(m) dm \\ & + \int_{M_{BM}}^{M_U} \psi(r, t - \tau_m) Q_{mi}(t - \tau_m) \phi(m) dm \\ & + X_{A_i} B(r, t), \end{aligned} \quad (6)$$

where $G_i(r, t) = [\sigma_g(r, t)X_i(r, t)]/\sigma_A(r)$, $\sigma_g(r, t)$ is the surface gas density, and $\sigma_A(r)$ is the present-time total surface mass density. X_{A_i} are the abundances in the infalling material, which is generally assumed to be primordial. $X_i(r, t)$ is the abundance by mass of the element i and Q_{mi} indicates the fraction of mass restored by a star of mass m in form of the element i , the so-called “production matrix” as originally defined by Talbot & Arnett (1973). We indicate with M_L the lightest mass which contributes to the chemical enrichment and it is set at $0.8M_\odot$; the upper mass limit, M_U , is set at $100M_\odot$.

For the IMF, we use that of Scalo (1986), constant in time and space. τ_m is the evolutionary lifetime of stars as a function of their mass m (Maeder & Meynet 1989).

The Type Ia SN rate has been computed following Greggio & Renzini (1983) and Matteucci & Greggio (1986) and it is expressed as:

$$R_{SNIa} = A_{Ia} \int_{M_{Bm}}^{M_{BM}} \phi(M_B) \left[\int_{\mu_m}^{0.5} f(\mu) \psi(t - \tau_{M_2}) d\mu \right] dM_B \quad (7)$$

where M_2 is the mass of the secondary, M_B is the total mass of the binary system, $\mu = M_2/M_B$, $\mu_m = \max[M_2(t)/M_B, (M_B - 0.5M_{BM})/M_B]$, $M_{Bm} = 3M_\odot$, $M_{BM} = 16M_\odot$. The IMF is represented by $\phi(M_B)$ and refers to the total

mass of the binary system for the computation of the Type Ia SN rate, $f(\mu)$ is the distribution function for the mass fraction of the secondary:

$$f(\mu) = 2^{1+\gamma}(1 + \gamma)\mu^\gamma \quad (8)$$

with $\gamma = 2$; A_{Ia} is the fraction of systems in the appropriate mass range, which can give rise to Type Ia SN events. This quantity is fixed to 0.05 by reproducing the observed Type Ia SN rate at the present time (Mannucci et al. 2005). Note that in the case of the Type Ia SNe the “production matrix” is indicated with Q_{mi}^{SNIa} because of its different nucleosynthesis contribution (for details see Matteucci & Greggio 1986 and Matteucci 2001).

We also apply the effect of radial inflows of gas on the model described in François et al. (2004).

We do not enter into details of this model, but we just remind here that in this case the Galaxy is assumed to have formed by means of two main infall episodes: the first formed the halo and the thick disk, the second the thin disk. (i.e. two-infall model) The typical time-scale for the formation of the halo is 0.8 Gyr and the entire formation period for the halo-thick disk does not last more than 2 Gyr. The time-scale for the thin disk is much longer, 7 Gyr in the solar vicinity, implying that the infalling gas forming the thin disk comes mainly from the intergalactic medium and not only from the halo (Chiappini et al. 1997). Moreover, the formation timescale of the thin disk is assumed to be a function of the galactocentric distance, leading to an inside-out scenario for the Galaxy disk build-up (eq. 3). The galactic thin disk is approximated by several independent rings, 2 kpc wide, without exchange of matter between them.

The main characteristic of the two-infall model is an almost independent evolution between the halo and the thin disk (see also Pagel & Tautvaisienne 1995). A threshold gas density of $7M_\odot pc^{-2}$ in the SF process (Kennicutt 1989, 1998, Martin & Kennicutt 2001) is also adopted for the disk. We consider for the halo a constant surface mass density as a function of the galactocentric distance at the present time equal to $17 M_\odot pc^{-2}$ and a threshold for the halo phase of $4 M_\odot pc^{-2}$ as it was assumed for the Model B in Chiappini et al. (2001).

The time-steps are small for the first 2 Gyr, of the order of $10^5 - 10^6$ years, then they become larger according to the smaller variation of the variables and reach values of the order of 1 Gyr.

3. Nucleosynthesis prescriptions

For the nucleosynthesis prescriptions of the O and Fe we adopt those suggested in François et al. (2004). They compared theoretical predictions for the [el/Fe] vs. [Fe/H] trends in the solar neighborhood for the above mentioned elements and they selected the best sets of yields required to best fit the data. In particular they found that the Woosley & Weaver (1995) metallicity dependent yields of SNe II provide the best fit to the data. No modifications are required for the yields of Ca, Fe, Zn and Ni as computed for solar chemical composition. For oxygen, the best results are given by the Woosley & Weaver (1995) yields computed as functions of the metallicity. For the other

elements, variations in the predicted yields are required to best fit the data (see François et al. 2004 for details).

Concerning O, the best agreement with the [O/Fe] vs. [Fe/H] and the solar O abundance, as measured by Asplund et al. (2009), is obtained by adopting the original Woosley & Weaver (1995) yields from massive stars as functions of metallicity. The same is not true for Fe: it was already known from the paper of Timmes et al. (1995) that the Fe yields as functions of metallicity overestimate the solar Fe and many people use those yields divided by a factor of 2. Alternatively, one can use the yields for solar chemical composition for the whole galactic lifetime and the result is the same, and this is what we do here.

Concerning the yields from Type SNeIa, revisions in the theoretical yields by Iwamoto et al. (1999) have been taken into account. The prescriptions for single low-intermediate mass stars are by van den Hoek & Groenewegen (1997), for the case of the mass loss parameter, which varies with metallicity (see Chiappini et al. 2003, model5).

4. The implementation of the radial inflow

Lacey & Fall (1985) showed that several mechanisms could drive a radial gas flow in the Galactic disk, We refer here to the possibility that the specific angular momentum of the infalling gas differs from the value for the circular motions in the disk. Therefore, mixing will induce a radial flow. Lacey & Fall (1985) suggested that a good estimate for velocity of that gas at 10 kpc is $v_R = -1 \text{ km s}^{-1}$. We implement radial inflows of gas on our reference model following the prescriptions described in Portinari & Chiosi (2000).

Let the k -th shell be defined by the galactocentric radius r_k , its inner and outer edge being labeled as $r_{k-\frac{1}{2}}$ and $r_{k+\frac{1}{2}}$. Through these edges, gas inflow with velocity $v_{k-\frac{1}{2}}$ and $v_{k+\frac{1}{2}}$, respectively. The flow velocities are taken positive outward and negative inward.

Radial inflows, with a flux $F(r)$, contribute to alter the gas surface density in the k -th shell in the following way:

$$\left[\frac{d\sigma_{gk}}{dt} \right]_{rf} = - \frac{1}{\pi \left(r_{k+\frac{1}{2}}^2 - r_{k-\frac{1}{2}}^2 \right)} \left[F(r_{k+\frac{1}{2}}) - F(r_{k-\frac{1}{2}}) \right] \quad (9)$$

where the gas flow at $r_{k+\frac{1}{2}}$ can be written as:

$$F(r_{k+\frac{1}{2}}) = 2\pi r_{k+\frac{1}{2}} v_{k+\frac{1}{2}} \left[\sigma_{g(k+1)} \right]. \quad (10)$$

As in Portinari & Chiosi (2000) we take the inner edge of the k -shell, $r_{k-\frac{1}{2}}$, at the midpoint between the characteristic radii of the shells k and $k-1$, and similarly for the outer edge $r_{k+\frac{1}{2}}$:

$r_{k-\frac{1}{2}} = (r_{k-1} + r_k)/2$, and $r_{k+\frac{1}{2}} = (r_k + r_{k+1})/2$. We get:

$$\left(r_{k+\frac{1}{2}}^2 - r_{k-\frac{1}{2}}^2 \right) = \frac{r_{k+1} - r_{k-1}}{2} \left(r_k + \frac{r_{k-1} + r_{k+1}}{2} \right). \quad (11)$$

Inserting eqs. (10) and (11) into eq. (9), we obtain the radial flow term to be added in eq. (6):

$$\left[\frac{d}{dt} G_i(r_k, t) \right]_{rf} = -\beta_k G_i(r_k, t) + \gamma_k G_i(r_{k+1}, t), \quad (12)$$

where β_k and γ_k are, respectively:

$$\beta_k = - \frac{2}{r_k + \frac{r_{k-1} + r_{k+1}}{2}} \times \left[v_{k-\frac{1}{2}} \frac{r_{k-1} + r_k}{r_{k+1} - r_{k-1}} \right] \quad (13)$$

$$\gamma_k = - \frac{2}{r_k + \frac{r_{k-1} + r_{k+1}}{2}} \left[v_{k+\frac{1}{2}} \frac{r_k + r_{k+1}}{r_{k+1} - r_{k-1}} \right] \frac{\sigma_{A(k+1)}}{\sigma_{Ak}}. \quad (14)$$

$\sigma_{A(k+1)}$ and σ_{Ak} are the actual density profile at the radius r_{k+1} and r_k , respectively. This formulation for the radial inflow follows the one used in Portinari & Chiosi (2000) but we want to stress that in the quantity β_k , concerning the term in square brackets, contains $r_{k+1} - r_{k-1}$ instead of $r_{k+1} + r_{k-1}$ as reported in the work of Portinari & Chiosi (2000), but certainly they used the right expression in their calculations. We assume that there are no flows from the outer parts of the disk where there is no SF. In our implementation of the radial inflow of gas, only the gas which resides inside the Galactic disk within the radius of 18 kpc can move inward by radial inflow. Our model is not subject to numerical instabilities up to 18 kpc. Therefore since we choose not to consider flows from galactocentric distances larger than 18 kpc, our results are not dependent on these instabilities.

5. Observational data

For the galactic abundance gradient of oxygen we use the following set of data: Deharveng et al. (2000), Esteban et al. (2005), Rudolph et al. (2006), who analyzed the Galactic HII Regions; Costa et al. (2004) who studied Planetary Nebulae (PNe); Andrievsky et al (2002a,b) who analyzed Galactic Cepheids. In order to compare our results with homogeneous sets of data, we separate the data by HII regions and PNe from the Cepheid ones. To better understand the trend of the data, we divide the data in 6 bins as functions of the galactocentric distance. In each bin we compute the mean value and the standard deviations for the studied elements. In Fig. 1 we report the whole collection of the data used in this paper. We are aware that there are some severe systematic uncertainties in each study that might justify larger error bars.

Concerning the data for the surface gas density profile and the SF rate along the Galactic disk we use the Dame et al. (1992) and Rana et al. (1991) ones.

6. The model results

In this section the results of both the two-infall model of Chiappini et al. (1997) and the one-infall model developed in this paper are presented. The two infall model can have an effect on the disk evolution but only at large galactocentric distances, as discussed in Chiappini et al. (2001).

We consider that in all models the efficiency of the SF is fixed at the value of $\nu = 1 \text{ Gyr}^{-1}$ in agreement with previous papers and in order to minimize the variation of model parameters.

In this paper we will focus on the effect of radial flows with different prescriptions for the infall and the SF rate. In Table 1 we summarize all the models we consider as a function of the

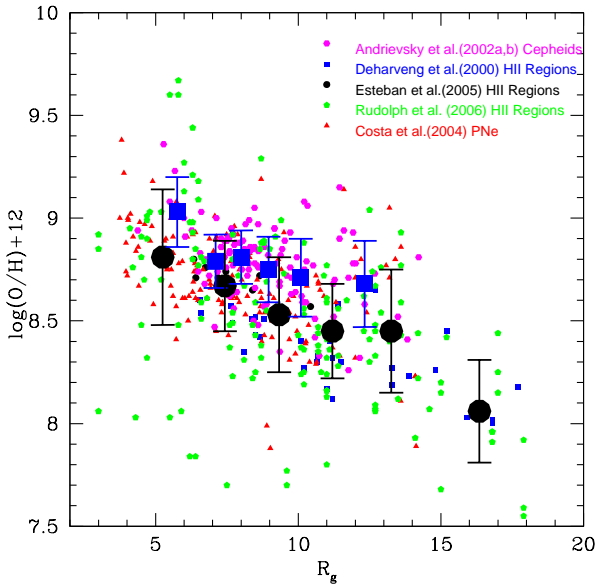


Fig. 1. Radial abundance gradient for oxygen from observations. The data are taken by Deharveng et al. (2000) (filled blue squares), Rudolph et al. (2006) (filled green pentagon), Costa et al. (2004) (red filled triangles), Andrievsky et al. (2002 a,b) (magenta filled hexagons), and Esteban et al. (2005) (black filled circles). We label with the large blue squared points the mean Cepheids values and relative error bars, whereas with the large black filled circles the mean values from the HII and Planetary Nebulae regions.

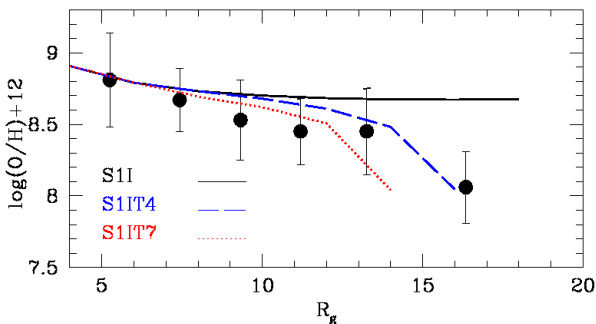


Fig. 2. Radial abundance gradient for oxygen. The black solid line refers to the one-infall model without threshold (S11), the blue long dashed line to a one-infall model with a threshold of $4 M_{\odot} pc^{-2}$ (S11T4) and the red dotted line a model with a threshold of $7 M_{\odot} pc^{-2}$ (S11T7). The filled circles and relative error bars are the observed values from HII regions and Planetary Nebulae.

type of infall, the timescale of the thin disk phase, the presence of the threshold, and the type of radial inflow. In particular, in the first column we report the model names, in the second the infall type, in the third in the fourth it is specified if there is inside-out formation (τ_D variable with the radius) and the threshold in the SF, respectively. Finally, in the fifth it is indicated the type of the implemented radial flow (only for the “no-static” models).

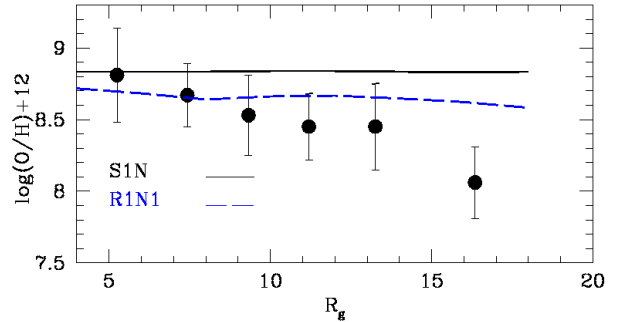


Fig. 3. Radial abundance gradient for oxygen. The black solid line refers to the one-infall model without threshold and with a constant $\tau_d = 4$ Gyr (S1N). The blue long dashed line represents the model with a radial inflow of 1 km/s (R1N1). The data are the same of Fig. 2.

First of all, we present the results obtained with the one-infall model with an inside-out formation. In Fig. 2 we show 3 different cases without radial flow: a model without threshold in the SF (S11), models S11T4 and S11T7 with a gas threshold for SF of 4 and $7 M_{\odot} pc^{-2}$, respectively, compared with the data from HII and PNe. We conclude that even if we consider a model with an inside-out formation the obtained gradient with a one-infall model without threshold is too flat and the observational data are not reproduced especially in the outer part of the Galaxy disk. We see instead that the slope for galactocentric distances between 4 and 14 kpc can be reproduced if we consider the model with a threshold in the SF. However, since the surface mass gas density in the outer parts of the disk is too small, there is no SF in this region and then no metals production and no chemical evolution.

Therefore, a possible solution to reproduce the data can be to consider a radial inflow of gas.

Portinari & Chiosi (2000) computed the effects of radial flows on their one-infall model without an inside-out formation. They adopted a unique timescale for disk formation irrespective of the galactocentric distance. Surprisingly, they found also in the case without radial flows an abundance gradient with a significant slope along the disk for the oxygen.

In the Fig. 3 we report the model S1N using the same prescriptions of the S11 model but without the inside-out formation, namely keeping τ_D constant along the Galaxy disk and equal to 4 Gyr. We find a flat gradient, and in the outer part of the disk the values of $\log(O/H)+12$ are even larger than the value in the inner part of the Galaxy. Portinari & Chiosi (2000) labeled S15a a model with the following main prescriptions: i) one-infall, ii) no threshold, iii) no inside-out. With these prescriptions they found a significant gradient along the Galactic disk of ~ -0.03 dex kpc^{-1} in contrast with our model result reported in Fig. 3 with the black solid line.

In Fig. 3 we also show the model R1N1 results where it was considered a constant speed of 1 km s^{-1} for the radial inflow on the one-infall model no threshold and no inside-out formation.

We see that the main effect of a migration of gas from the outer part of the Galaxy toward the inner part without thresh-

Table 1. The list of the models described in this work. The first letter in the model names is S if that model is a “static” one, otherwise R if we show a model with radial flow of gas. The follow number (1 or 2) is related to the number of infall, the letter I is for the case for inside-out model and N for a constant formation time scale along the disk. When we consider a threshold in the star formation we label that with a T. The last letter in the names of models with radial flow is related to the speed of the radial flow.

Models	Infall type	τ_d	Threshold	Radial inflow
S1I	1 infall	1.033 R (kpc) -1.27 Gyr	no	/
S1N	1 infall	4 Gyr	no	/
S1IT4	1 infall	1.033 R (kpc) -1.27 Gyr	$4 M_{\odot}\text{pc}^{-2}$	/
S1IT7	1 infall	1.033 R (kpc) -1.27 Gyr	$7 M_{\odot}\text{pc}^{-2}$	/
S2IT	2 infall	1.033 R (kpc) -1.27 Gyr	$7 M_{\odot}\text{pc}^{-2}$ (thin disk phase) $4 M_{\odot}\text{pc}^{-2}$ (halo thick disk phase)	/
R1I1	1 infall	1.033 R (kpc) -1.27 Gyr	no	-1 km s^{-1}
R1N1	1 infall	4 Gyr	no	-1 km s^{-1}
R1IL	1 infall	1.033 R (kpc) -1.27 Gyr	no	linear inflow pattern
R1IT01	1 infall	1.033 R (kpc) -1.27 Gyr	$4 M_{\odot}\text{pc}^{-2}$	-0.1 km s^{-1}
R1IT05	1 infall	1.033 R (kpc) -1.27 Gyr	$4 M_{\odot}\text{pc}^{-2}$	-0.5 km s^{-1}
R2ITV	2 infall	1.033 R (kpc) -1.27 Gyr	$7 M_{\odot}\text{pc}^{-2}$ (thin disk phase) $4 M_{\odot}\text{pc}^{-2}$ (halo thick disk phase)	variable inflow pattern

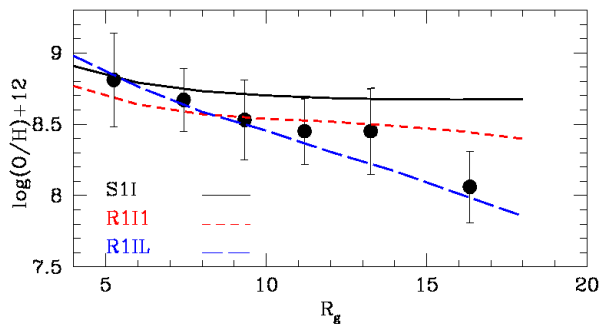


Fig. 4. Radial abundance gradient for oxygen. The black solid line refers to the one infall model without threshold and with the inside-out formation (S1I). The red short dashed line represents the model with a radial inflow of 1 km s^{-1} (R1I1) and the blue long dashed line the best fit model using a variable velocity for the radial inflow (R1IL). The data are the same of Fig. 2

old and inside-out is to produce a weak abundance gradient ($\sim -0.014 \text{ dex kpc}^{-1}$) at variance with observations. In our model with a constant radial velocity of the flow, the abundance of oxygen at each galactocentric distance is lower than the values found for the S1N model; this is due to the fact that the metals tend to be stored in the very central parts ($R < 5 \text{ kpc}$) of the Galaxy and that we used a constant speed of the radial flow. In fact, Schönrich & Binney (2009) considered both the stellar and gas flows in a chemical evolution model considering a model without inside-out formation. They were able to fit

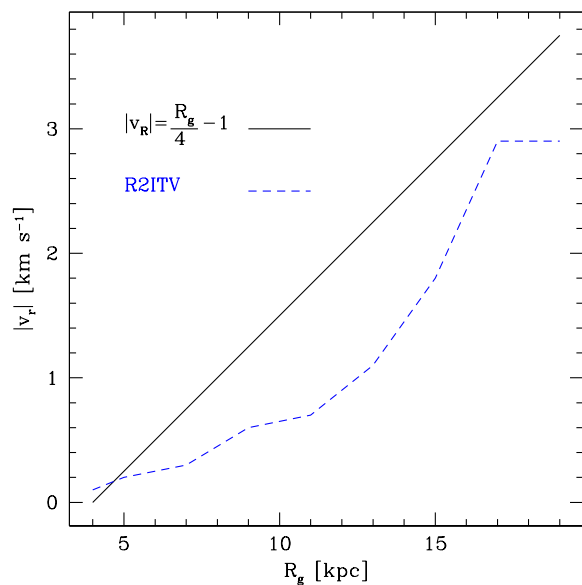


Fig. 5. With the solid line we show the requested pattern of the velocity to reproduce the observed gradient as a function of the galactocentric distance for the R1IL model, with the dashed line for the R2ITV. In this plot we show the modulus of the radial inflow velocity as a function of the galactocentric distance.

the observed data including a variable speed of the gas flow by means of two free parameters, a situation where each ring may have its own velocity.

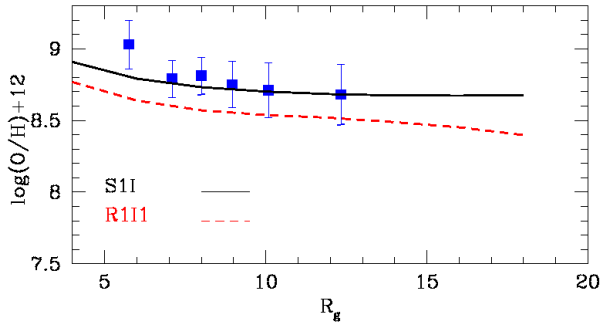


Fig. 6. Radial abundance gradient for oxygen. The black solid line refers to the one infall model without threshold and with the inside-out formation (S1I). The red short dashed line represents the model with a radial inflow of 1 km s^{-1} (R1I1). The data are mean values and relative errors from Cepheids by Andrievsky et al. (2002a,b).

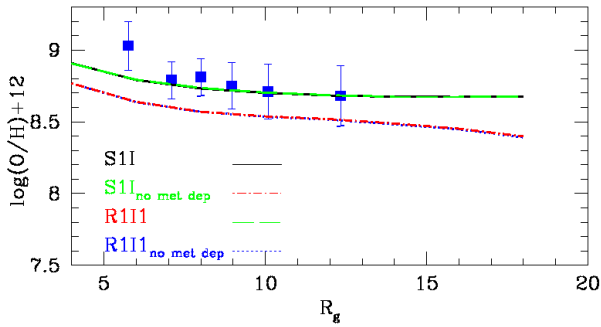


Fig. 7. Radial abundance gradient for oxygen. The black solid line refers to the one infall model without threshold and with the inside-out formation (S1I) with metallicity dependent yields, the green long dashed line is the case with solar yields. The red short dashed dotted line represents the model with a radial inflow of 1 km s^{-1} (R1I1) with metallicity dependent yields and the blue long dashed line with solar yields. The data are mean values and relative errors from Cepheids by Andrievsky et al. (2002a,b).

We remind that also the S1I model with inside-out formation using the law described in eq. (3) and no threshold is not able to reproduce the set of data for the outer part of the disk. Then we tried to find a best fit to the observed data varying the velocity of the gas flow. In Fig. 4 we report the R1I1 model results with a constant radial flow along the Galactic disk fixed at -1 km s^{-1} and model with an inflow velocity variable in space which results to be R1IL. We see that the model with the constant radial flow has a steeper gradient compared to S1I but there are still problems in reproducing the outer region of the Galaxy. To reproduce the data we need a variable velocity for the inflow of gas. With the model R1ITL we are able to fit quite well the data of HII regions and PNe assuming a linearly increasing flow velocity towards the outer regions as shown in Fig. (5). We recall that the case of a linearly increasing flow velocity was also studied in the work of Goetz & Köppen (1992).

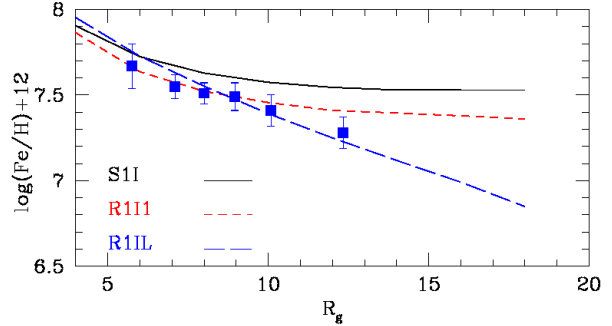


Fig. 8. Radial abundance gradient for iron. The black solid line refers to the one infall model without threshold and with the inside-out formation (S1I). The red short dashed line represents the model with a radial inflow of 1 km s^{-1} (R1I1), and the blue long dashed line the best fit model using a variable velocity for the radial inflow (R1IL). The mean values and relative errors from Cepheids by Andrievsky et al. (2002a,b) are reported with filled blue squares.

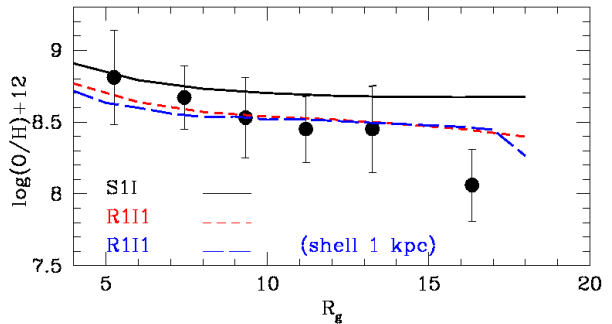


Fig. 9. Radial abundance gradient for oxygen. The black solid line refers to the one infall model without threshold and with the inside-out formation (S1I). The red short dashed line represents the model with a radial inflow of 1 km s^{-1} (R1I1) using shells 2 kpc wide and the blue long dashed line label the same physical parameters but running a model with shells 1 kpc wide. The data are mean values and relative errors from Cepheids by Andrievsky et al. (2005a,b).

In Fig. 5 we show the pattern of the linear velocity we adopted to reproduce the observed gradient as a function of the galactocentric distance for the one-infall model. The range of velocities in modulus span the range $0-4 \text{ km s}^{-1}$ in accordance with the results of Schönrich & Binney (2009).

In Fig. 6 we compare the models S1I and R1I1 with the data from Cepheids. We note that, since the observed gradient for these objects is almost flat, both models can easily reproduce it.

We recall that in our calculations we consider the nucleosynthesis prescription used in François et al. (2004), therefore for oxygen we use metallicity dependent yields. To ascertain how the choice of metal dependent yields affects radial flows, in Fig. 7 we run the same models of Fig. 6 but in the case of solar yields for oxygen. We note that the reference models as

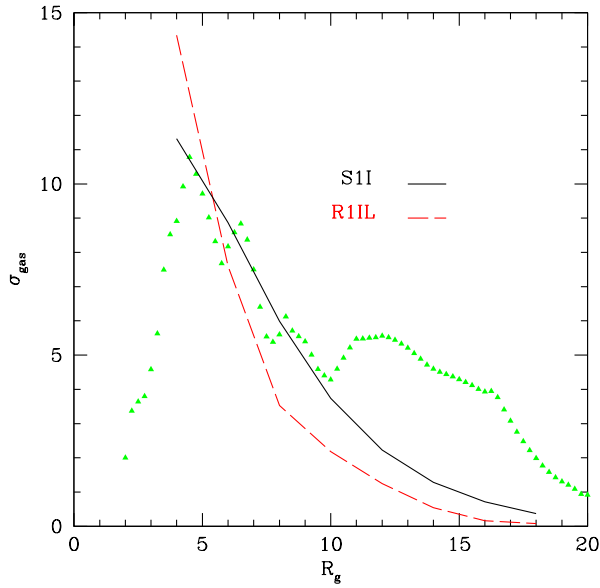


Fig. 10. The surface gas density profile as a function of the radial distance for the reference one-infall model S1I drawn with the black solid line and for the best fit model R1IL. The green filled triangles represents the data of Dame et al (1993).

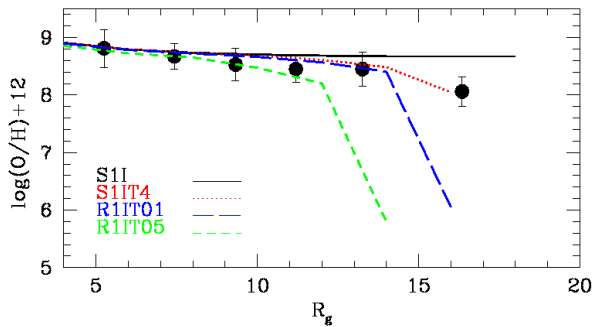


Fig. 11. Radial abundance gradient for oxygen. The black solid line refers to the one-infall model without threshold and with the inside-out formation (S1I). The red short dashed line represents the model with a threshold of $4 M_{\odot} pc^{-2}$ (S1IT4), the blue long dashed line the model with a threshold of $4 M_{\odot} pc^{-2}$ combined to a radial inflow of 0.1 km s^{-1} (R1T01), the green dotted line the model with a threshold of $4 M_{\odot} pc^{-2}$ combined inflow of 0.5 km/s (R1T05). The data are the same of Fig. 2.

well as the ones with radial flows, give exactly the same results for metal dependent and solar yields concerning the abundance gradients. This result is expected since the present time abundances in the ISM are the result of the global production of a given element; metal dependent yields vary with the metallicity but the global production of an element is the same as for solar metallicity yields since in both cases the solar abundances (i.e. the ISM abundances 4.5 Gyr ago) are reproduced.

In Fig. 8 we show the results of models S1I, R1I1, and R1IL for iron. We note that iron shows a steeper gradient when compared with oxygen one, because of the different time-scales involved in the production of these two elements.

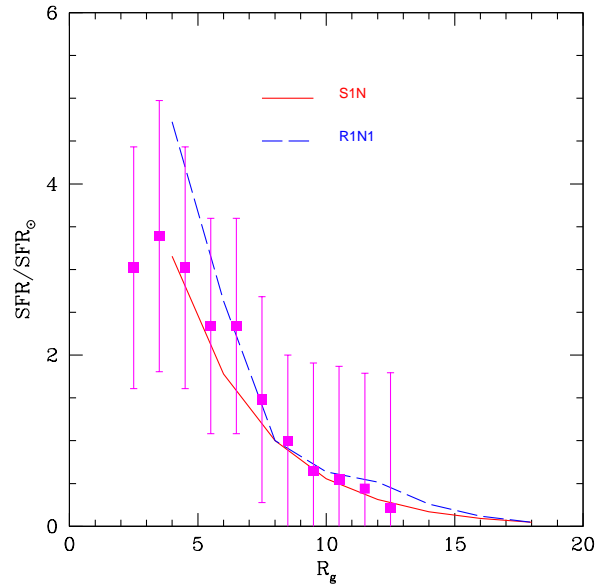


Fig. 12. The SF rate normalized to the solar values as a function of the galactocentric distance for the one-infall model with no inside-out formation. The data are taken by Rana et al. (1991) and are reported with the magenta points and relative error bars, with the red solid line we report the reference static model S1N whereas the dashed blue line is the model with a radial inflow of -1 km s^{-1} (R1N1).

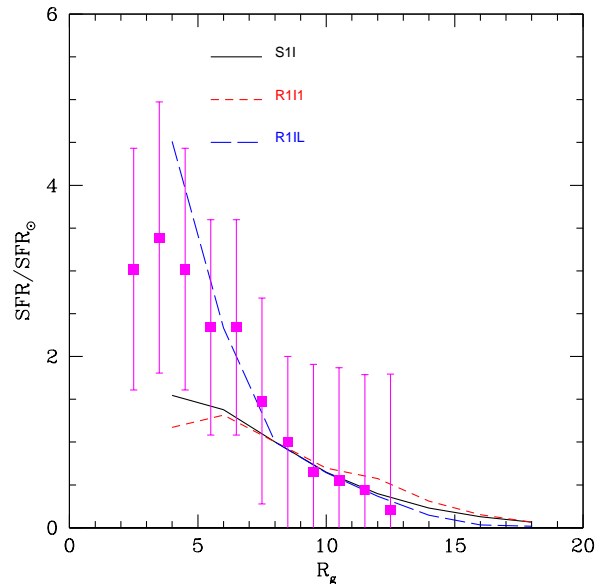


Fig. 13. The SF rate normalized to the solar values as a function of the galactocentric distance for the one-infall model with inside-out formation. The data are taken by Rana et al. (1991) and are reported with the magenta points and relative error bars, with the black solid line we report the reference static model S1I whereas the red short dashed line is the model with a radial inflow of -1 km s^{-1} (R1I1) and the blue long dashed line is the best fit radial inflow model (R1IL).

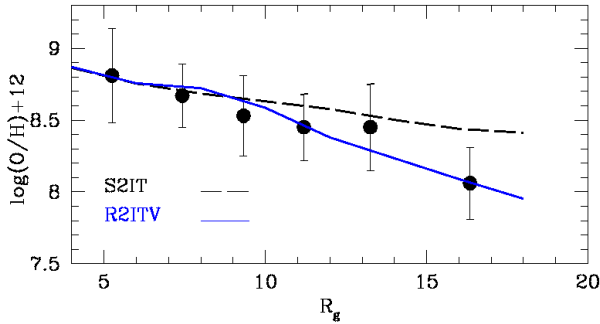


Fig. 14. Radial abundance gradient for oxygen. The black long dashed line refers to the two-infall model S2IT. The blue solid line represents the the best 2 infall fit model using a variable velocity for the radial inflow (R2ITV). The data are the same of Fig. 2

In our calculations we assume that: i) there is no inflow from the outer parts of the disk ($R > 20$ kpc), ii) our shells are 2 kpc wide.

The point ii) is consistent with the fact that on smaller scales other processes must be important. In fact, in Spitoni et al. (2008) we proved that galactic fountains can affect abundance gradients only on scales smaller than 1 kpc. Here we test how the choice of a finer resolution affects our results. In Fig. 9 the model R1I1 is considered both for shells 1 and 2 kpc wide. We note that differences arise only in the outer part of the disk, because of the adopted method for the implementation of radial inflows. It is worth noting that choosing a smaller shell does not affect our results expect for distances $R > 17$ kpc and not in a substantial way as shown in Fig. 9.

We pass now to analyze how the profile of the gas along the Galactic disk is modified with the variable velocity pattern used for the best fit of the abundance gradient. In the Fig. 10 we compare the results of model S1I and R1IL for what concerns the gas surface density profile as a function of the radial distance.

We note that both models underestimates the gas for distances > 10 kpc and do not reproduce the peak and the decrease of gas for $R < 5$ kpc. This is probably due to the bar which is not considered in our model.

We want also to stress that a model without a threshold in the SF has problems to reproduce the values in outer part of the disk. We also test a model in which we combine the effect of a threshold in the SF plus a radial inflow. In Fig. 11 is shown the “static” model S1IT4 with the “mixed models” considering both the threshold and the radial inflow. We fixed a threshold value at $4 M_{\odot} \text{ pc}^{-2}$ considering 2 constant speed radial inflows: the model RI1T01 with a velocity of 0.1 km s^{-1} and the model RI1T05 with a velocity 0.5 km s^{-1} , respectively. A velocity of 0.5 km/s is high enough to put system under threshold already at the radial distance of 16 kpc, whereas the model without radial flow but with a threshold of $4 M_{\odot} \text{ pc}^{-2}$ has no chemical evolution for $R > 16$ kpc.

We want also to test how the radial inflows of gas affect the SF rate along the disk of the Galaxy. In Fig. 12 we report the

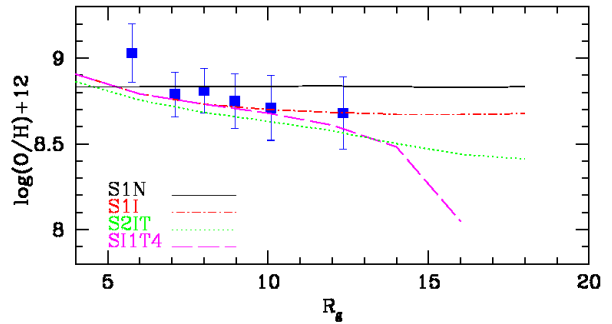


Fig. 15. Radial abundance gradient for oxygen for the models S1N (black solid line), S1I (red dotted dashed line), and S2IT (green dotted line), and S1IT4 (magenta long dashed line). The data collection from Cepheids are reported.

results for the S1N and the R1N1 models, whereas in Fig. 13 the results with inside-out formation: S1I, R1I1 and R1IL models. In these Figs. we show the SF rate normalized to the solar value as a function of the galactocentric distance. Because of the uncertainties in this data set, as evident from the big error bars, we cannot draw firm conclusions. Having said that, we can however draw some considerations. In Fig. 12 both models well fit the data for the SF rate, whereas in Fig. 13 models S1I and R1I1 underestimate the $\text{SFR}/\text{SFR}_{\odot}$ for $R < 8$ kpc. On the other hand, the model R1IL fits perfectly the $\text{SFR}/\text{SFR}_{\odot}$ ratio in the range 6 - 18 kpc. For galactocentric distances smaller than 6 kpc the R1IL model overestimates the mean $\text{SFR}/\text{SFR}_{\odot}$, but our results are inside the 1 sigma error bar, because of the uncertainty in the data. We do not show our model results for galactocentric distances smaller than 4 kpc because in this region the effects of the central bar might be important and our model is built only for the disk and not for the bulge area.

In this part we study the effects of a radial inflow on the two-infall model described in Sect. 2. In Fig. 14 we see that our two-infall reference model S2IT is able to give rise to a steep gradient for oxygen but not enough to reproduce the data set. We also show the model R2ITV with a varying velocity pattern for the radial inflow velocity. In the case of the two-infall model we are not anymore able to fit the abundance gradient for oxygen using a simple constant relation between radial infall velocity and galactocentric distance, then we consider a pattern where the velocity starting from 17 kpc decreases monotonically toward the center part of the Galaxy (see Fig. 5).

From Fig. 5 we note that the range of velocities required to fit the data is quite similar to the one used for the one-infall model.

In Fig. 15 we report the data from Cepheids compared with standard models without radial flows (S1N, S1I, S1IT4, S2IT). We see that all the models with inside-out formation show a rather shallow slope for the oxygen abundance gradient compatible with the Cepheid data. In Fig. 16 we compare standard models without radial flows with all data sets considered in this paper. In conclusion, if we use only the data of the Cepheids, the abundance gradient is not so steep and it can be reproduced without any radial inflow.

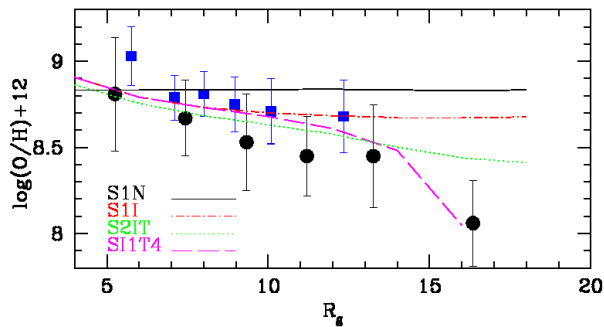


Fig. 16. Radial abundance gradient for oxygen for the models S1N (black solid line), S1I (red dotted dashed line), and S2IT (green dotted line), and S1IT4 (magenta long dashed line). The data collection from Cepheids (blue squares) and from HII regions (black circles) are reported.

7. Conclusions

In this paper we have studied the effects of radial inflows of gas on a detailed chemical evolution model. We also reported some results of the metals gradients obtained with “static” models considering different prescriptions for the infall law and star formation. Our main conclusions can be summarized as follows:

- If we consider the one-infall model with an inside-out formation (τ_D varying with the radius) the obtained gradient without threshold is too flat and the observational data are not reproduced especially in the outer part of the Galaxy disk. The slope for intermediate galactocentric distances can be reproduced if we consider the model with a threshold. However, since the surface gas mass density in the outer part of the disk is too small, there is no star formation in this region and then no metals production and no chemical evolution.
- Taking into account a constant τ_D along the Galaxy disk equal to 4 Gyr, we find a flat gradient in contrast with the work of Portinari & Chiosi (2000) where a gradient along the Galactic disk of ~ -0.03 dex kpc^{-1} was found.
- A constant radial inflow with speed of 1 km s^{-1} (not expected theoretically) applied to the one-infall model with no threshold and no inside-out produces a weak abundance gradient (~ -0.014 dex kpc^{-1}) and the metals tend to be stored in the very central parts of the Galaxy.
- The required pattern of the radial flow velocity varies linearly with the galactocentric distance and spans a range between 0 and 4 km/sec. This conclusion holds for the one-infall model without threshold and with inside-out formation.
- Our “static” two-infall model with a threshold in the star formation and the inside-out formation is able to give rise to a steep gradient but not enough to reproduce the data set. The required pattern of the radial inflow velocity (in modulus) to reproduce the observed gradient is quite similar to the one of the one-infall model.

- If we use the data of the Cepheids the observed abundance gradient is not so steep and can be reproduced with our “static” reference models without any radial inflow.
- As shown first in Götz & Köppen (1992), then in Portinari & Chiosi (1999) and Colavitti et al. (2008), a variable efficiency in the star formation rate if coupled with an inside-out formation can also reproduce the abundance gradient. Since this variable efficiency in the Milky Way is observationally motivated (Marcon-Uchida et al. 2010), it should not be disregarded as source of the abundance gradients. Moreover, as we have shown, to reproduce the abundance gradients by means of radial flows we need a specific variable speed of the flow, and at this moment there are not observational constraints for the speed of this flow of gas along the disk of the Galaxy.
- Finally, we conclude that radial gas flows can be in principle important to reproduce the gradients along the disk, although an inside-out formation coupled with variable efficiency of star formation and threshold in gas density can also well reproduce the data without radial flows. Probably, all these processes are present in the Galactic disk: in order to decide which of these processes would prevail in the formation of the disk, we need more detailed data both on the abundance, gas and star formation rate gradients, as well as data on high redshift disks.

Acknowledgements. We thank the referee for the enlightening suggestions. We also thank G. Cescutti, and S. Recchi for many useful discussions. We acknowledge financial support from PRIN 2007 MUR Prot. No. 2007JJC53X-001.

References

- Andrievsky, S.M., Bersier, D., Kovtyukh, V. V. et al 2002a, A&A, 384, 140
- Andrievsky, S.M., Kovtyukh, V.V., Luck R.E. et al 2002b, A&A, 381, 32
- Asplund, M., Grevesse, N., Sauval, A. J., Scott, P., 2009, ARA&A, 47, 481
- Bertin G., Lin C.C., 1996, *Spiral structure in galaxies – A density wave theory*, MIT Press, Cambridge, Massachusetts
- Cescutti, G., Matteucci, F., Francois, P., & Chiappini, C. 2007, A&A, 462, 943
- Cescutti, 2008, A&A, 481, 691
- Chiappini C., Matteucci F., & Gratton R., 1997, ApJ, 477, 765
- Chiappini C., Matteucci F., & Meynet G., 2003, ApJ, 410, 257
- Chiappini C., Matteucci F., & Romano D., 2001, ApJ, 554, 1044
- Colavitti. E., Cescutti, G., Matteucci F., Murante G., 2009, A&A, 496, 429
- Costa, R. D. D., Uchida, M. M. M., & Maciel, W. J. 2004, A&A, 423, 199
- Dame, T. M., 1992, AIPCP, 278, 267
- Deharveng, L., Peña, M., Caplan, J., & Costero, 2000, MNRAS, 311, 329
- Esteban, C., Garca-Rojas, J., Peimbert, M., Peimbert, A., Ruiz, M. T., Rodriguez, M., Carigi, L., 2005, ApJ, 618, 95
- François P., Matteucci F., Cayrel R., Spite, M., Spite, F., & Chiappini, C., 2004, A&A, 421, 613

- Götz, M., Köppen, J., 1992, *A&A*, 262, 455
- Greggio L., & Renzini A., 1983, *A&A*, 118, 217
- Kennicutt, R. C., Jr., 1989, *ApJ*, 344, 685
- Kennicutt, R. C., Jr., 1998, *ApJ*, 498, 541
- Iwamoto, K., Brachwitz, F., Nomoto, K., et al. 1999, *ApJ* Suppl. Ser. 125, 439
- Lacey C.G., Fall M., 1985, *ApJ*, 290, 154
- Maeder, A., & Meynet, G., 1989, *A&A*, 210, 155
- Mannucci, F., Della Valle, M., Panagia, N., Cappellaro, E., Cresci, G., Maiolino, R., Petrosian, A., & Turatto, M, 2005, *A&A*, 433, 807
- Marcon-Uchida, M.M., Matteucci, F., Costa, R.D.D., 2010, arXiv:1004.4139
- Martin, C. L., & Kennicutt, R. C., Jr., 2001, *ApJ*, 555, 301
- Matteucci, F., 2001, *The Chemical Evolution Of The Galaxy*, Kluwer Academic Publishers.
- Matteucci, F., & François, P., 1989, *MNRAS*, 239, 885
- Matteucci M.F., Greggio L., 1986, *A&A*, 154, 279
- Mayor M., Vigroux L., 1981, *A&A* 98, 1
- Pagel, B.E.J., & Tautvaisiene, G., 1995, *MNRAS*, 276, 505
- Portinari L., Chiosi C., 1999, *A&A* 350, 827
- Portinari, L., Chiosi, C., 2000, *A&A*, 355, 929
- Rana, N. C. 1991, *ARA&A*, 29, 129
- Rudolph, A. L., Fich, M., Bell, G.R., Norsen, T., Simpson, J.P., Haas, M.R., & Erickson, E.F., 2006, *ApJS*, 162, 346
- Scalo, J. M., 1986, *FCPh*, 11, 1
- Schmidt, M., 1959, *ApJ*, 129, 243
- Schönrich, R., & Binney, J, 2009, *MNRAS*, 396, 203
- Sommer-Larsen J., Yoshii Y., 1990, *MNRAS*, 243, 468
- Spitoni, E., Recchi, S., Matteucci, F., 2008. *A&A*, 484, 743
- Talbot, R., J., Jr., Arnett, W., D., 1973, 186, 51
- Thon R., Meusinger H., 1998, *A&A*, 338, 413
- Timmes, F.X., Woosley, S.E., Weaver, T.A., 1995, *ApJS*, 98, 617
- van den Hoek L.B., & Groenewegen M.A.T. 1997, *A&A* Suppl., 123, 305
- Woosley S.E., & Weaver, T.A., 1995, *ApJ*, 101, 181